

1  
2  
3  
4  
5  
6  
7  
8  
9  
10  
11  
12  
13  
14  
15  
16  
17  
18  
19  
20  
21  
22  
23  
24  
25  
26  
27  
28  
29  
30  
31  
32  
33  
34  
35  
36  
37  
38  
39  
40  
41  
42  
43  
44  
45  
46  
47  
48  
49  
50  
51  
52  
53  
54  
55  
56  
57  
58  
59  
60  
61  
62  
63  
64  
65

## A Plug Release Mechanism for Membrane Permeation by MLKL

### Supplementary Figures.

**Figure S1.** The extra residues in MLKL(2-178) do not alter the overall structure of MLKL(2-154). **A.** Superposition of  $^1\text{H}$ - $^{15}\text{N}$  HSQC spectra of MLKL(2-154) (black) and MLKL(2-178) (red). The spectra are the same shown in Figure 1 but were plotted at lower contour levels to enable observation of the weaker cross-peaks from MLKL(2-178). Selected cross-peaks that are markedly shifted and or broadened when comparing the two spectra are labeled with the corresponding residue number. The inset shows a ribbon diagram of the structure of MLKL(2-154) described here (in blue) with the residues labeled on the  $^1\text{H}$ - $^{15}\text{N}$  HSQC spectra colored in yellow. Note that all these residues are near the C-terminus (labeled C). **B.**  $^1\text{H}$ - $^{15}\text{N}$  HSQC spectrum of MLKL(2-154) showing assignment of selected well-resolved cross-peaks. Related to Figure 1.

**Figure S2.** Liposome co-floatation assays with MLKL(2-154). The assays were performed with liposomes containing different percentages of cardiolipin (CL) as indicated above the lanes. Samples were analyzed by SDS PAGE and coomassie blue staining. The positions of molecular weight markers (kDa) are indicated on the right. Related to Figure 2.

**Figure S3.** MLKL(2-154) does not cause membrane fusion. The bar diagrams illustrate dynamic light scattering data obtained for liposomes under the conditions of the leakiness assays

1  
2  
3  
4 described in Figure 3, in the absence (**A**) and presence (**B**) of 150 nM MLKL(2-154). The  
5  
6 average radii ( $R$ ) and polydispersity (%Pd) yielded by the data are indicated. Related to Figure 3.  
7  
8  
9

10  
11 **Figure S4.** Sequence alignment of the MLKL N-terminal domains. An alignment of the  
12  
13 sequences of the N-terminal domains of MLKL from different species is shown, with selected  
14  
15 residue numbers corresponding to the human sequence above the alignment. Residues are color-  
16  
17 coded as follows: red, small plus hydrophobic (excluding Tyr); blue, acidic; magenta, basic plus  
18  
19 His; green, polar plus Gly. The alignment was prepared with Clustal Omega  
20  
21 (<http://www.ebi.ac.uk/Tools/msa/clustalo/>). Related to Figure 4.  
22  
23  
24  
25  
26  
27

28  
29 **Figure S5.** Effects of mutagenesis and NBD labeling on the liposome leakage activity of  
30  
31 MLKL(2-154). **A.** CD spectra of 2  $\mu$ M MLKL(2-154) in 20 mM sodium phosphate pH 7.4, 100  
32  
33 mM NaCl, in the absence (black) and presence (red) of liposomes (1 mM lipids) with the same  
34  
35 lipid composition used for leakiness assays. **B.** Liposome leakage assays performed as in Figure  
36  
37 3 with 2  $\mu$ M MLKL(2-154) in the absence (black) and presence (red) of 1 mM DTT. **C,D.**  
38  
39 Liposome leakage assays in the presence of WT MLKL(2-154) (black curve), and the indicated  
40  
41 NBD labeled mutants. Proteins were added after 200 s. The data were normalized with the  
42  
43 fluorescence observed after adding detergent, and setting at zero the fluorescence right before  
44  
45 protein addition. Related to Figure 5.  
46  
47  
48  
49  
50  
51  
52

53 **Figure S6.** Complementary analysis of packing between helices in the MLKL N-terminal region.  
54  
55 **A.** Helices H2 and H5 in the crystal structure of MLKL (Murphy et al., 2013). The atoms of the  
56  
57 side chains of basic residues are colored in blue and those of acidic side chains are colored in  
58  
59  
60  
61  
62  
63  
64  
65

1  
2  
3  
4 red. In other side chains and the backbone, carbon atoms are in green, oxygen atoms are in red,  
5  
6 nitrogen atoms are in blue and sulfur atoms are in yellow. The helices are indicated at the  
7  
8 bottom. Note the poor packing between the two helices. **B.** Two-dimensional  $^1\text{H}$ - $^1\text{H}$  strip from a  
9  
10 three-dimensional  $^1\text{H}$ - $^{13}\text{C}$  NOESY-HSQC spectrum of MLKL(2-154) taken at the  $^{13}\text{C}$  chemical  
11  
12 shift corresponding to W109 HH2. Cross-peak assignments are indicated on the right. **C.** Ribbon  
13  
14 and stick model of the region containing the W109 side chain in the solution structure of  
15  
16 MLKL(2-154). Residues with protons near the W109 HH2 proton are labeled. Related to Figure  
17  
18  
19  
20  
21 6.  
22  
23  
24  
25

26 **Figure S7. A.** Superposition of  $^1\text{H}$ - $^{15}\text{N}$  HSQC spectra of MLKL(2-154) (black) and MLKL(2-  
27  
28 123) (red). **B.** Liposome co-floatation assays with MLKL(2-154), MLKL(2-123), MLKL(2-  
29  
30 154)K26E,R30E and MLKL(2-154)K22Q,K25Q. The assays were performed with liposomes  
31  
32 containing 15% cardiolipin (CL). Samples were analyzed by SDS PAGE and coomassie blue  
33  
34 staining. The positions of molecular weight markers (kDa) are indicated on the right. **C.** Ribbon  
35  
36 diagram showing the region where part of helix H6 packs against helix H4. Side chains are  
37  
38 shown as stick models with carbon atoms in green, oxygen atoms in red, nitrogen atoms in blue  
39  
40 and sulfur atoms in yellow. The side chains of C86 from helix H4 and F148 from helix H6 are  
41  
42 labeled. Related to Figure 7.  
43  
44  
45  
46  
47  
48  
49  
50  
51  
52  
53  
54  
55  
56  
57  
58  
59  
60  
61  
62  
63  
64  
65

1  
2  
3  
4  
5  
6  
7  
8  
9  
10  
11  
12  
13  
14  
15  
16  
17  
18  
19  
20  
21  
22  
23  
24  
25  
26  
27  
28  
29  
30  
31  
32  
33  
34  
35  
36  
37  
38  
39  
40  
41  
42  
43  
44  
45  
46  
47  
48  
49  
50  
51  
52  
53  
54  
55  
56  
57  
58  
59  
60  
61  
62  
63  
64  
65

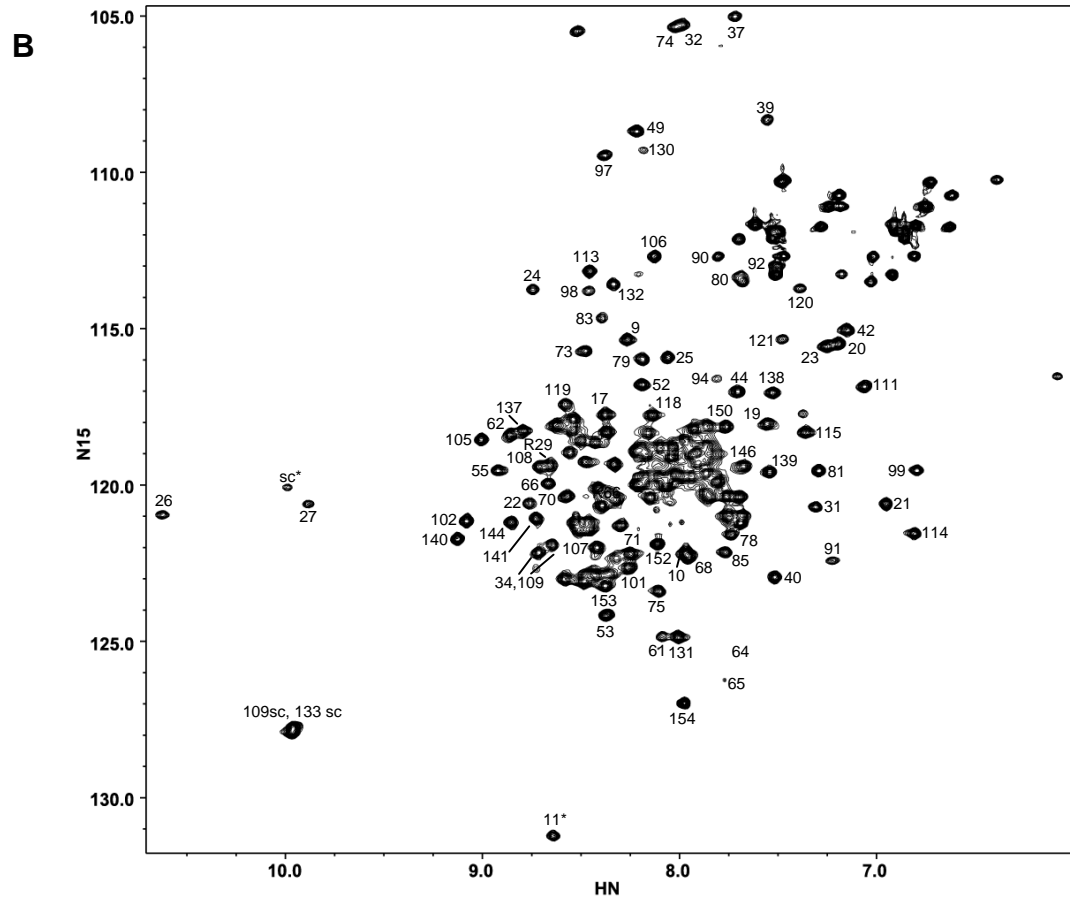
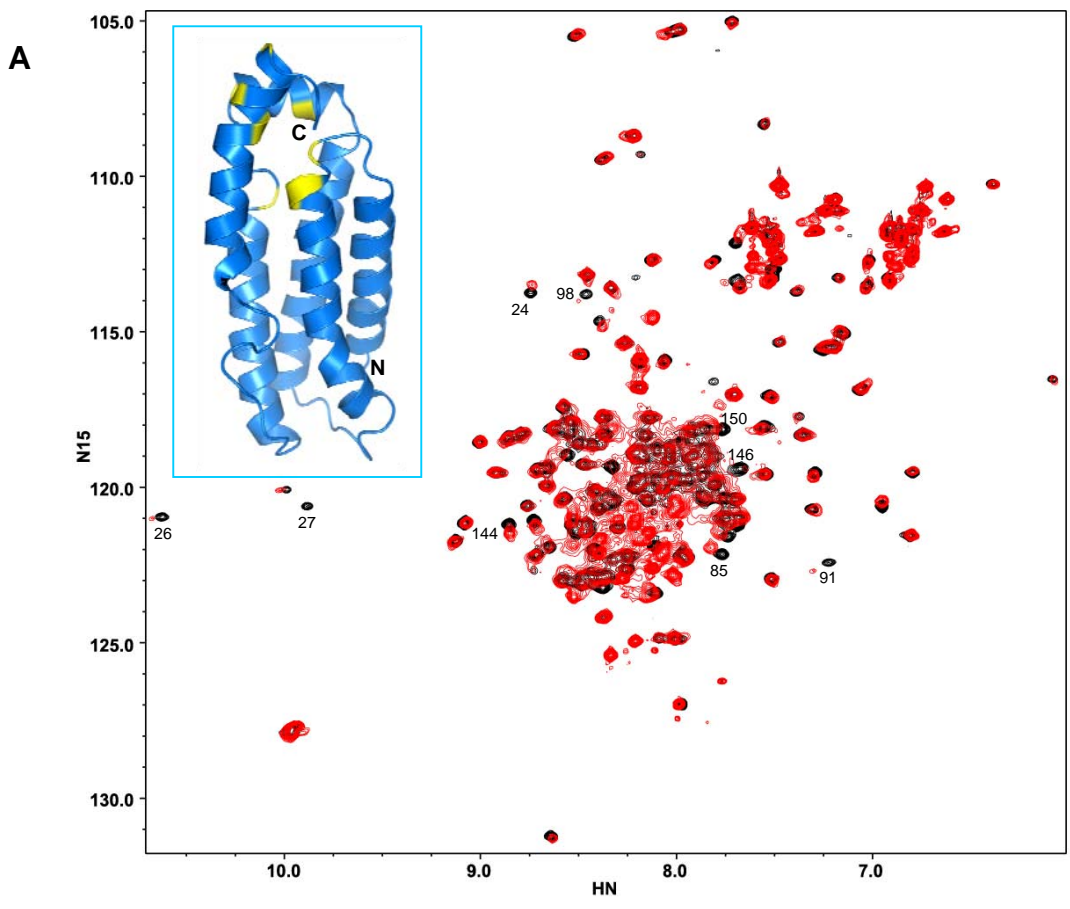


Figure S1  
Su et al.

1  
2  
3  
4  
5  
6  
7  
8  
9  
10  
11  
12  
13  
14  
15  
16  
17  
18  
19  
20  
21  
22  
23  
24  
25  
26  
27  
28  
29  
30  
31  
32  
33  
34  
35  
36  
37  
38  
39  
40  
41  
42  
43  
44  
45  
46  
47  
48  
49  
50  
51  
52  
53  
54  
55  
56  
57  
58  
59  
60  
61  
62  
63  
64  
65

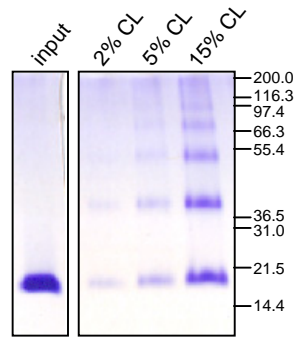


Figure S2  
Su et al.

1  
2  
3  
4  
5  
6  
7  
8  
9  
10  
11  
12  
13  
14  
15  
16  
17  
18  
19  
20  
21  
22  
23  
24  
25  
26  
27  
28  
29  
30  
31  
32  
33  
34  
35  
36  
37  
38  
39  
40  
41  
42  
43  
44  
45  
46  
47  
48  
49  
50  
51  
52  
53  
54  
55  
56  
57  
58  
59  
60  
61  
62  
63  
64  
65

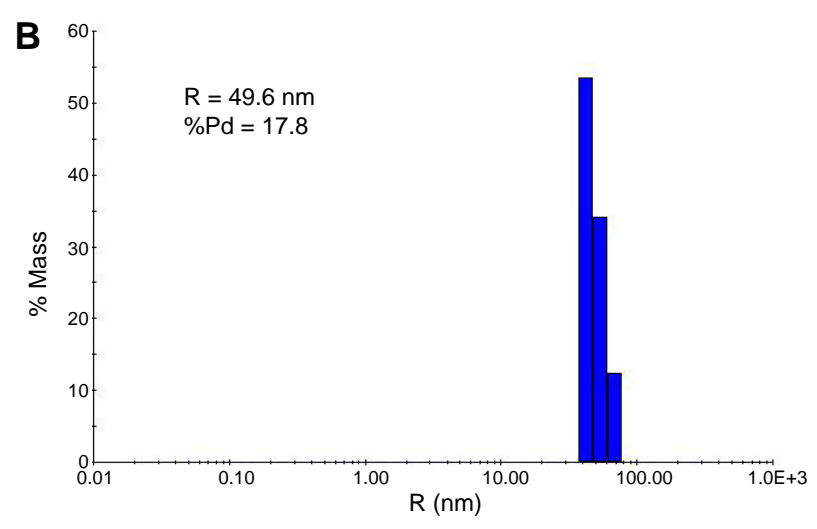
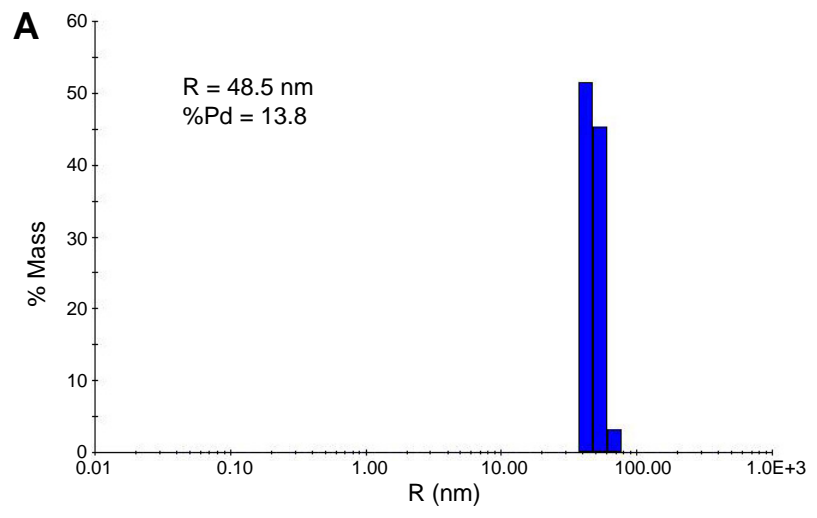


Figure S3  
Su et al.

1  
2  
3  
4  
5  
6  
7  
8  
9  
10  
11  
12  
13  
14  
15  
16  
17  
18  
19  
20  
21  
22  
23  
24  
25  
26  
27  
28  
29  
30  
31  
32  
33  
34  
35  
36  
37  
38  
39  
40  
41  
42  
43  
44  
45  
46  
47  
48  
49  
50  
51  
52  
53  
54  
55  
56  
57  
58  
59  
60  
61  
62  
63  
64  
65

**A**

```
Callorhynchus_milii 1          21          41  
MECVDKICSLALAIYKLCDEVKENRNQCRLRIRIEVLTESVKTITEQKLTGDFTD-IGK  
Myotis_davidii     MDILKNVISAAQYVYQLCEKMQHCEGQYKRLRNRIHGLLQPLQELQARGEENLSPG-IIT  
Camelus_ferus      MDQLGQIISLGQLIYKQTEEMKYCQKQCQRLGNRVHGLLQPLQMLQAQGERNLSPQ-ITI  
Mus_musculus       MDKLGQIIKLQQLIYEQCEKMKYCRKQCQRLGNRVHGLLQPLQRLQAQGKKNLPDD-ITA  
Homo_sapiens       MENLKHIIITLGQVIHKRCEEMKYCKKQCRRLGHRVGLGLIKPLEMLQDQGKRSVPSEKLT  
Pan_troglodytes    MENLKHIIITLGQVIHKRCEEMKYCKKQCRRLGHRVGLGLIKPLEMLQDQGKRSVPSEKLT  
* : : . : . . . : : : : : . * : * * * * : * : : : : : : : : : :  
  
Callorhynchus_milii 61          81          101  
VLKELVETLRTTEHYIKRFTEGHKFCCKWFNAYKFKDHFELNERNLNDAAQALGLALQTEQ  
Myotis_davidii     ALNNFQAALAEAKKIDKFSDKPFLHKFLKSGKNKELFTDVNNRLTDVHQELSLALQVYQ  
Camelus_ferus      ALSHFQAALAEAKERIDKFSNKSNIHKFLTAGQDRILFSGVKNSLRDAWEELSLLLQVHQ  
Mus_musculus       ALGRFDEVLKEANQQIEKFSKSHIWKFVSVGNDKILFHEVNEKLRDVWEELELLQLQVYH  
Homo_sapiens       AMNRFKAALAEANGEIEKFSNRSNICRFLTASQDKILFKDVNRKLSDVWKELSLLLQVEQ  
Pan_troglodytes    AMNRFKAALAEANGEIEKFSNRSNICRFLTASQDKILFKDVNRKLSDVWKELSLLLQVEQ  
. : . : . * . : : * : * * : : : : : : : * : * . * * . : * * * * . :  
  
Callorhynchus_milii 121         141  
VVQLKSIFKAETRRKKEDKEDSEKDARDLDKLMKE  
Myotis_davidii     GVSISSISK-EDWKQEDQQDAEEDWRAFQNLTAE  
Camelus_ferus      WRHTSSISPGAAWQEDQQDAEEDRQVIERLRSG  
Mus_musculus       WNTVSDVSPASWQEDRQDAEEDGN-----  
Homo_sapiens       RMPVSPISQGASWAQEDQQDADEDRAAFQMLRRD  
Pan_troglodytes    RMPVSPISQGASWAQEDQQDADEDRAAFQMLRRD  
. : : : * * * * * * * * .
```

Figure S4  
Su et al.

1  
2  
3  
4  
5  
6  
7  
8  
9  
10  
11  
12  
13  
14  
15  
16  
17  
18  
19  
20  
21  
22  
23  
24  
25  
26  
27  
28  
29  
30  
31  
32  
33  
34  
35  
36  
37  
38  
39  
40  
41  
42  
43  
44  
45  
46  
47  
48  
49  
50  
51  
52  
53  
54  
55  
56  
57  
58  
59  
60  
61  
62  
63  
64  
65

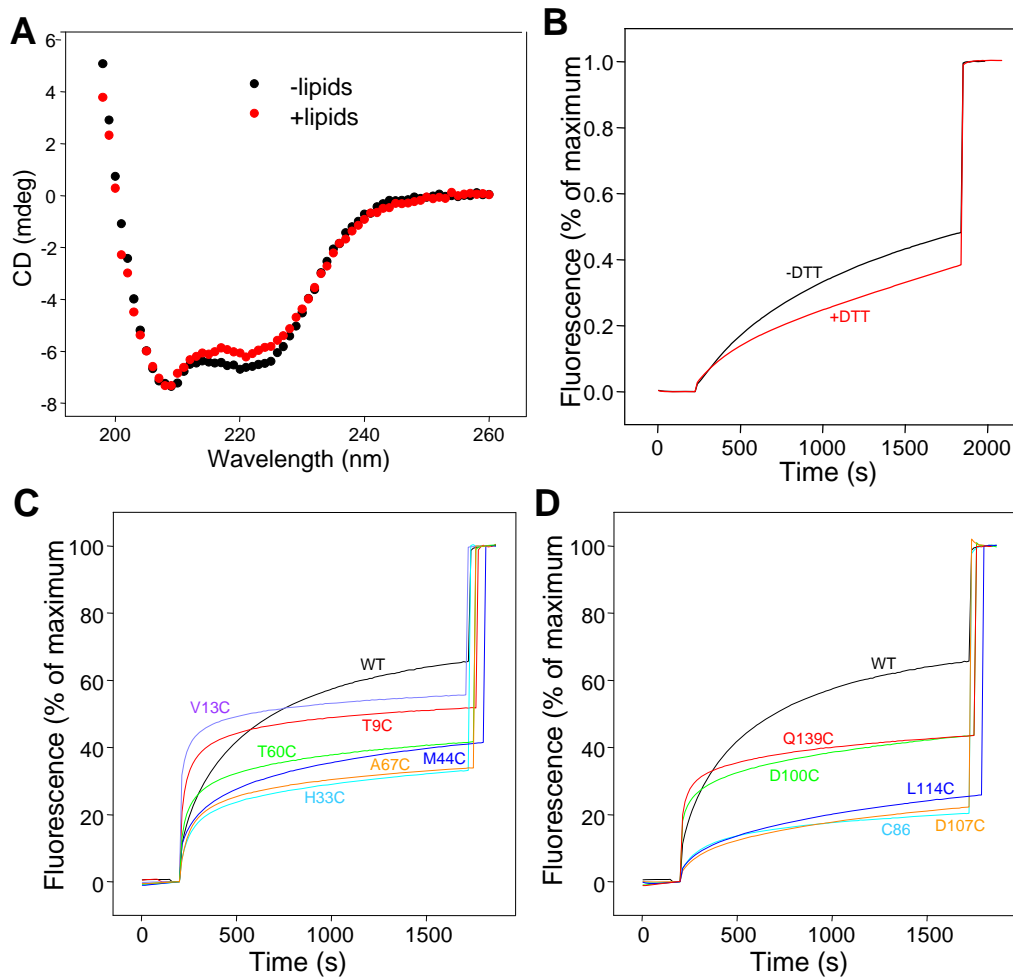


Figure S5  
Su et al.



1  
2  
3  
4  
5  
6  
7  
8  
9  
10  
11  
12  
13  
14  
15  
16  
17  
18  
19  
20  
21  
22  
23  
24  
25  
26  
27  
28  
29  
30  
31  
32  
33  
34  
35  
36  
37  
38  
39  
40  
41  
42  
43  
44  
45  
46  
47  
48  
49  
50  
51  
52  
53  
54  
55  
56  
57  
58  
59  
60  
61  
62  
63  
64  
65

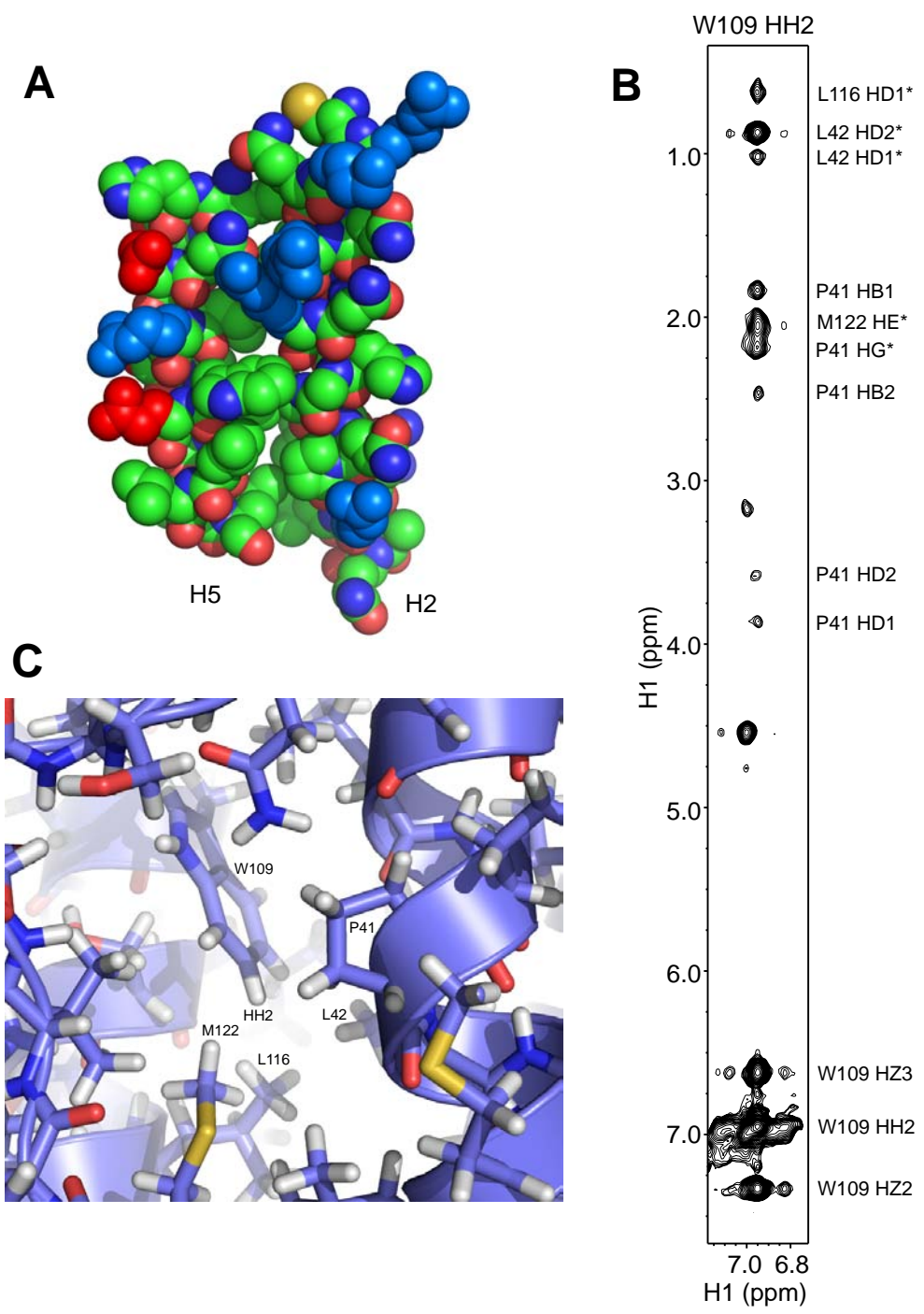


Figure S6  
Su et al.

1  
2  
3  
4  
5  
6  
7  
8  
9  
10  
11  
12  
13  
14  
15  
16  
17  
18  
19  
20  
21  
22  
23  
24  
25  
26  
27  
28  
29  
30  
31  
32  
33  
34  
35  
36  
37  
38  
39  
40  
41  
42  
43  
44  
45  
46  
47  
48  
49  
50  
51  
52  
53  
54  
55  
56  
57  
58  
59  
60  
61  
62  
63  
64  
65

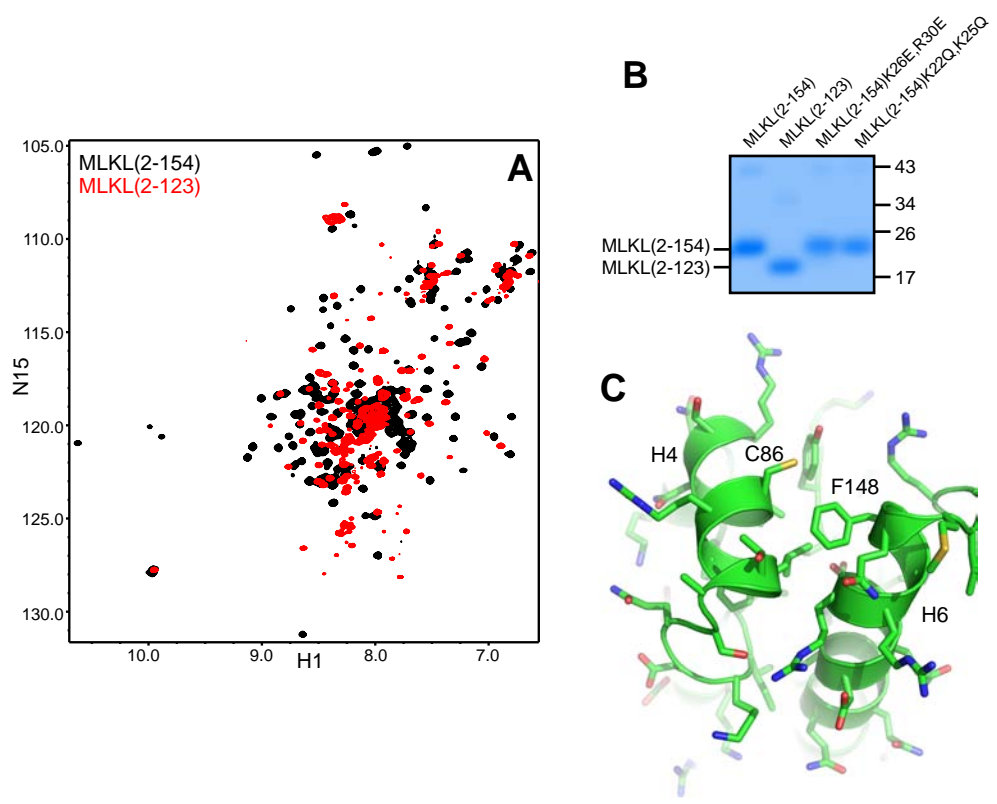


Figure S7  
Su et al.

## Supplementary Experimental Procedures

### NMR spectroscopy

Initial  $^1\text{H}$ - $^{15}\text{N}$  HSQC spectra of MLKL(2-123) (50  $\mu\text{M}$ ), MLKL(2-154) (200  $\mu\text{M}$ ) and MLKL (2-178) (200  $\mu\text{M}$ ) were acquired at 600 MHz on INOVA or DD2 spectrometers equipped with cold probes (Agilent), using samples dissolved in 20 mM HEPES (pH 7.0), 150 mM NaCl. For analysis of binding to nanodiscs and liposomes,  $^1\text{H}$ - $^{15}\text{N}$  HSQC spectra were acquired at 800 MHz on an INOVA800 spectrometer equipped with a cold probe (Agilent) with samples dissolved in 20 mM HEPES (pH 7.4), 100 mM NaCl. The protein concentrations were 20-50  $\mu\text{M}$  and the total lipid concentrations were 1 mM. Nanodiscs of 12 nm diameter containing 45% 1-palmitoyl-2-oleoyl-*sn*-glycero-3-phosphocholine (POPC), 30% 1-palmitoyl-2-oleoyl-*sn*-glycero-3-phosphoethanolamine (POPE), 10% L- $\alpha$ -phosphatidylinositol (PI) and 15% cardiolipin were prepared as described (Brewer et al., 2011). Liposomes for NMR experiments contained the same lipid composition and were prepared as described below for the leakage assays.

### Liposome co-floitation assays

Liposomes with lipid composition of 58% POPC, 30% POPE, 10% PI and 2% cardiolipin; 55% POPC, 30% POPE, 10% PI and 5% cardiolipin; or 45% POPC, 30% POPE, 10% PI and 15% cardiolipin, were prepared as described above for the dye leakage assays. Liposome samples containing 2 mM lipids were first incubated with 5  $\mu\text{M}$  MLKL(2-154) at room temperature for 1 hour. The proteins bound to the liposomes were separated from the unbound proteins by floatation on a Histodenz density gradient (40%:35%:30%) as described (Guan et al., 2008).

1  
2  
3  
4 After centrifugation, the proteins bound to the liposomes that migrated to the top of the gradient  
5  
6 were taken (30  $\mu$ l) and analyzed by SDS-PAGE and Coomassie blue staining.  
7  
8  
9

## 10 11 **NBD fluorescence experiments**

12  
13 To label MLKL (2-154) at specific places with NBD, the four endogenous cysteines (C18, C24,  
14  
15 C28 and C86) were first mutated to serines. Single cysteine mutations were then introduced into  
16  
17 the six different helices of MLKL(2-154): T9C, V13C, H33C, M44C, T60C, A67C, D100C,  
18  
19 D107C, L114C and Q139C. The C86 MLKL(2-154) mutant was made by mutating only the  
20  
21 other three native cysteines of MLKL(2-154) (C18, C24 and C28). For labeling with NBD, 100  
22  
23  $\mu$ M solutions of the mutants were incubated with 1 mM NBD-maleimide (IANBD amide;  
24  
25 Invitrogen) in a buffer containing 20 mM HEPES pH7.2, 100 mM NaCl, 200  $\mu$ M TCEP at room  
26  
27 temperature for 2 hours. The samples were then incubated with 20 mM DTT at room temperature  
28  
29 for 15 min to quench the free NBD-maleimide. The NBD-labeled protein samples were then  
30  
31 separated from the free NBD-maleimide by gel filtration using Superdex 200 10/30 with a buffer  
32  
33 containing 20 mM HEPES pH7.4, 100 mM NaCl.  
34  
35  
36  
37  
38  
39  
40

41 Liposomes (5 mM) with lipid composition of 45% POPC, 30% POPE, 10% PI and 15%  
42  
43 cardiolipin were prepared as described above for the leakage assays but without sulforhodamine  
44  
45 B. To study the insertion of the NBD probes of the different mutants into the membrane, NBD  
46  
47 fluorescence emission (500-650 nm) spectra were acquired with samples containing 0.2  $\mu$ M  
48  
49 NBD-labeled protein samples without or with 300  $\mu$ M lipid vesicles in buffer containing 20 mM  
50  
51 HEPES (pH 7.4) and 100 mM NaCl. The experiments were performed at room temperature on a  
52  
53 PTI spectrofluorimeter with excitation at 485 nm.  
54  
55  
56  
57  
58  
59  
60  
61  
62  
63  
64  
65

1  
2  
3  
4  
5  
6  
7  
8  
9  
10  
11  
12  
13  
14  
15  
16  
17  
18  
19  
20  
21  
22  
23  
24  
25  
26  
27  
28  
29  
30  
31  
32  
33  
34  
35  
36  
37  
38  
39  
40  
41  
42  
43  
44  
45  
46  
47  
48  
49  
50  
51  
52  
53  
54  
55  
56  
57  
58  
59  
60  
61  
62  
63  
64  
65

**Supplementary References**

Guan,R., Dai,H., and Rizo,J. (2008). Binding of the Munc13-1 MUN Domain to Membrane-Anchored SNARE Complexes. *Biochemistry* 47, 1474-1481.